RESEARCH ARTICLE

Blood Science

OPEN

Enhancing hemophilia A gene therapy by strategic F8 deletions in AAV vectors

Juan-Juan Zhao[a,b], Sai-Ning Tian[c], Xiang Li[a,b], Zu-Yi Peng[c], Guo-Hua Li[a,b], Feng Zhang[a,b], Mei Zhao[a,b], Jian-Ping Zhang[a,b,*], Xiao-Bing Zhang[a,b,c,*]

[a]State Key Laboratory of Experimental Hematology, National Clinical Research Center for Blood Diseases, Haihe Laboratory of Cell Ecosystem, Institute of Hematology & Blood Diseases Hospital, Chinese Academy of Medical Sciences & Peking Union Medical College, Tianjin 300020, China; [b]Tianjin Institutes of Health Science, Tianjin 301600, China; [c]Haihe Laboratory of Cell Ecosystem, Tianjin Medical University, Tianjin, China

Abstract

Hemophilia A, caused by a deficiency in factor VIII (F8), is a promising target for gene therapy. This study aims to enhance the efficacy of adeno-associated virus serotype 8 (AAV8) vectors, specifically those encoding B-domain-deleted F8 (BDDF8), to treat the condition. We focused on improving therapeutic outcomes by strategically deleting amino acids at the furin cleavage site (RHQR), a modification that is crucial for increasing F8 expression and reducing capsid stress during vector packaging. Using computational modeling with AlphaFold2, combined with western blotting and in vivo clotting assays, we developed and tested several AAV8-BDDF8 variants in a hemophilia A mouse model. The AAV8-BDDF8-ΔRHQR10 variant, which includes a 10-amino acid deletion at the RHQR site, demonstrated a 2- to 3-fold increase in F8 activity, with sustained expression and no hepatotoxicity. This variant also showed reduced capsid stress and enhanced protein expression. However, the observed decline in long-term efficacy highlights the ongoing challenges in AAV-F8 gene therapy, emphasizing the need for continuous improvements. Our findings offer valuable insights for refining AAV-mediated gene therapy in hemophilia A, showing that targeted molecular modifications can significantly enhance therapeutic performance while ensuring safety.

Key Words: Adeno-associated viruses (AAV); BDDF8; Gene therapy; Hemophilia A

1. INTRODUCTION

Hemophilia A, the most common form of hemophilia, is a genetic disorder caused by a deficiency in clotting factor VIII (F8), which is essential for proper blood coagulation. It usually results from mutations in the F8 gene, leading to reduced production and function of the F8 protein.[1–3] The current standard treatment involves regular infusions of recombinant or plasma-derived F8. However, this approach is limited by several challenges, including high costs, frequent administration, and the risk of immune responses, such as the development of inhibitors that reduce treatment efficacy.[4–6] These challenges highlight the urgent need for more sustainable and efficient therapeutic alternatives.

Gene therapy with adeno-associated virus (AAV) vectors offers a promising solution, as AAV can infect both dividing and non-dividing cells, has low immunogenicity, and supports long-term gene expression.[7,8] This is especially relevant for hemophilia A, where continuous F8 expression in the liver—the primary site of synthesis—could provide a durable treatment. The use of AAV8 vectors, which show high liver tropism, is promising for enhancing clinical outcomes in hemophilia A.[9,10] The selection of specific promoters, such as the liver-specific transthyretin (TTR) promoter, is crucial for achieving high expression levels of the therapeutic gene primarily in hepatocytes, reflecting natural F8 synthesis patterns while minimizing unwanted immune responses and off-target effects.[11]

Innovations in computational biology have identified cis-acting regulatory modules (CRMs) that considerably boost liver-targeted gene expression, potentially enhancing the safety and efficacy of treatments by allowing for lower vector doses.[12–14] Consequently, this study incorporates CRMs into AAV vectors to investigate their effect on F8 gene expression.

*Address correspondence: Xiao-Bing Zhang, No. 10 Yuexin Road, High-tech Zone, Binhai New Area, Tianjin, China. E-mail address: zhangxbhk@gmail.com (X.-B. Zhang); Jian-Ping Zhang, E-mail address: zhangjianping@ihcams.ac.cn (J.-P. Zhang).

Conflict of interest: The authors declare that they have no conflict of interest.

J.-J.Z. and S.-N.T. contributed equally as the first author.

This work was supported by the National Key Research and Development Program of China (Grant Nos. 2019YFA0110803, 2019YFA0110204, 2019YFA0110802, and 2021YFA1100900), the National Natural Science Foundation of China (Grant Nos. 82402188, 81870149, 82070115, 81770198, 81890990, and 81730006), the Chinese Academy of Medical Sciences (CAMS) Innovation Fund for Medical Sciences (CIFMS) (Grant Nos. 2024-I2M-3-018, 2023-I2M-2-007, 2022-I2M-2-001, 2022-I2M-2-003, 2021-I2M-1-041, 2021-I2M-1-040, and 2021-I2M-1-001), the Non-profit Central Research Institute Fund of Chinese Academy of Medical Sciences (Grant No. 2020-PT310-011), the Tianjin Synthetic Biotechnology Innovation Capacity Improvement Project (Grant No. TSBICIP-KJGG-017), the CAMS Fundamental Research Funds for Central Research Institutes (Grant No. 3332021093), the Haihe Laboratory of Cell Ecosystem Innovation Fund (Grant Nos. 24HHXBSS00005 and HH22KYZX0022), and the State Key Laboratory of Experimental Hematology Research Grant (Grant No. Z23-05).

Materials supporting the findings of this paper are available from the corresponding author upon reasonable request.

Blood Science (2025) 7, 1–9:e00217.

Received July 20, 2024; Accepted December 6, 2024.

http://dx.doi.org/10.1097/BS9.0000000000000217

The F8 gene, approximately 7.1 kb long, encodes an inactive single-chain polypeptide that undergoes cleavage to become a functional cofactor in blood clotting. Furin-mediated cleavages at specific sites are essential for F8 activation and function. After secretion, the B-domain of F8, which accounts for 40% of the protein, is removed, allowing F8 to function effectively without it.[15] In gene therapy, shortened F8 variants are used to fit within AAV vector limitations, while preserving essential functionality.[16] Recent studies have illuminated the B-domain's role in modulating intracellular interactions and secretion, pointing to its potential involvement in activation and clearance processes.[17,18]

Building on this knowledge, our study explores additional deletions adjacent to the furin cleavage site to potentially enhance vector packaging efficiency and therapy outcomes. Specifically, we investigated variants lacking the RHQR sequence and surrounding residues while preserving essential N-linked glycosylation sites, critical for F8's secretion and function.[19–21] Our modifications aimed to create a more compact F8 gene that could be effectively packaged within AAV vectors, potentially leading to improved therapeutic efficacy. Through extensive experimentation, we identified several new F8 variants that demonstrated heightened activity and functionality, suggesting promising directions for clinical gene therapy in treating hemophilia A.

2. METHODS

2.1. AAV plasmid design and assembly

We developed the pAAV-CRM8-TTR-BDDF8-N6 (ALBss) plasmid by utilizing custom-designed primers for polymerase chain reaction (PCR) amplification of the required DNA fragments. The vector components were amplified from existing laboratory plasmids through the utilization of the highly efficient KAPA HiFi polymerase (KAPA Biosystems, Wilmington, Massachusetts). Subsequently, the GeneJET Gel Extraction Kit (Thermo Fisher Scientific, Waltham, Massachusetts) was utilized to meticulously purify these amplified components. The PCR-generated fragments were then integrated into full-fledged plasmids in strict accordance with the detailed protocol of the NEBuilder HiFi DNA Assembly Kit.[22,23] For the initial validation phase, restriction enzyme digestion was implemented. Subsequently, a comprehensive sequencing approach, incorporating both Sanger and nanopore technologies, was adopted. The Sanger sequencing provided high-accuracy base reading for short sequences, while the nanopore sequencing offered long-read capabilities, jointly ensuring the unambiguous confirmation of the precise DNA sequence of each variant.

2.2. AAV8 vector production and purification

HEK293T cells were cultured in 15 cm dishes until they reached 80% to 90% confluency. Transfection was performed using a PEIMax-DNA mixture in serum-free DMEM, containing the pAAV-Helper Plasmid (Cell Biolabs, Inc., San Diego, California), AAV Rep-Cap Plasmid, and the plasmid carrying the target gene at a 2:1:1 ratio. A total of 40 μg of DNA and 80 μg of PEIMax were applied per dish, followed by a 20-minute incubation before transfection. Cell lysis occurred 5 days post-transfection using a chemical lysis buffer supplemented with 20 units/mL of benzonase (SCBT) for 2 hours to reduce nucleic acid contamination. Subsequently, the lysate underwent centrifugation at 5000 g for a duration of 10 minutes to retrieve the AAV particle-laden supernatant which was sterile filtered through a 0.22 μm filter.[24,25] A Minimate system (300-kDa cut-off) concentrated viral particles. Purification was completed by iodixanol gradient ultracentrifugation, followed by dialysis in phosphate-buffered saline (PBS) containing 0.05% Pluronic F68 using a Vivaspin 20 concentrator (100 kDa MWCO) to remove residual iodixanol. Viral titers were gauged by droplet digital PCR (ddPCR), and aliquots were stored at −80°C to prevent degradation.[26]

2.3. AlphaFold2 protein prediction

Protein structural predictions were performed using the AlphaFold2 platform available on AlphaFold Colab (https://colab.research.google.com), configured for GPU acceleration.[27] The mature protein sequence, excluding the signal peptide, was input into the "query-sequence" field to focus on the functional portion of the protein. Each sequence was uniquely labeled for tracking purposes. The prediction was initiated by selecting "Run all," generating multiple structural model files named "ranked_*.pdb," which were sorted by confidence levels. The highest confidence model was selected for further analysis. Structural similarities were evaluated using the TM-align tool[28] to compare the new BDDF8-N6 variant models with standard controls, such as baseline BDDF8-N6. TM scores near 1 indicate high similarity, while scores closer to 0 suggest low similarity.[29,30]

2.4. In Cellulo assessment of BDDF8 variants

BDDF8 variants were evaluated in Hepa 1-6 cells, cultured in Dulbecco's Modified Eagle Medium (DMEM, Gibco, Waltham, Massachusetts) supplemented with 10% fetal bovine serum (FBS, Gibco). Cells were maintained at 70% to 80% confluency for 24 hours before transduction to ensure optimal growth conditions. AAV8-F8 vectors were added at a multiplicity of infection (MOI) of 1,000,000, based on virus titration results. After inoculation, cells were incubated at 37°C. Twenty-four hours post-transduction, cells were washed with PBS (Gibco) to remove unbound viral particles and cultured for an additional 2 days. The secretion of BDDF8 into the culture supernatant can be detected by Western blotting to assess F8 protein expression.

2.5. Western blot analysis for BDDF8 protein

Seventy-two hours post-transduction, supernatants from Hepa 1-6 cells were collected and centrifuged at low temperature at a high speed for 10 minutes to remove cellular debris. Proteins were denatured by heating with 5× sodium dodecyl sulfate (SDS) sample buffer at 100°C for 5 minutes. To ensure consistent protein amounts, the total protein concentration in the supernatant was quantified and adjusted for equal loading. Sodium dodecyl sulfate polyacrylamide gel electrophoresis (SDS-PAGE) was performed on a 12% polyacrylamide gel, starting at 60 V until the dye front reached the separating gel, followed by an increase to 120 V to fully resolve the proteins. Proteins were separated by electrophoresis and then transferred onto a nitrocellulose (NC) membrane (Solarbio Science & Technology Co., Ltd., Beijing, China) at 100 V via a semi-dry transfer system. After blocking the non-specific binding sites, the F8 protein was labeled with a sheep anti-human F8 primary antibody (Thermo Fisher; PA1 - 43045) diluted at 1:1000. Subsequent to 3 rounds of Tris-Buffered Saline with Tween 20 (TBST) rinsing, the rabbit anti-sheep IgG secondary antibody conjugated with horseradish peroxidase (HRP) (ABClonal; AS023) diluted at a ratio of 1:10,000 was applied. After the rinsing process, the bands were detected by employing a chemiluminescent substrate (ECL) system. Band intensities were captured and analyzed using ImageJ software[31] and normalized to the ~80 kDa band of a protein marker (Genscript Biotech Corporation, Piscataway, New Jersey; M00624) to determine relative expression levels of the various AAV-BDDF8-N6 variants. The commercially available

F8 protein (Xyntha; Wyeth Pharmaceuticals, Madison, New Jersey) served as a positive control.

2.6. Intravenous injection of AAV vectors

A 6- to 8-week-old hemophilia A mouse model with a targeted F8 exon 16 knockout was utilized to closely simulate the human disease phenotype, which is marked by a severe lack of F8 and an F8 activity of less than 1% This model has been extensively validated in our laboratory and others for evaluating the efficacy and safety of F8 supplementation therapies, facilitating the translation of results to potential clinical applications.[32] All animal procedures were performed in accordance with ethical guidelines and approved by the SKLEH Institutional Animal Care and Use Committee and the Institute of Hematology. The injection volume for each mouse was determined based on the ddPCR-measured titer of the AAV vector and the mouse's body weight, ensuring the volume did not exceed 10% of the mouse's weight. To mitigate bleeding risks, 0.5 IU of F8 protein (Xyntha; Wyeth Pharmaceuticals) was administered before the injection. The AAV vector was delivered via tail vein injection over approximately 3 to 4 seconds for controlled administration. Blood samples were taken from the lateral tail vein at regular intervals for subsequent analysis.

2.7. Immunosuppression

Methylprednisolone and cyclophosphamide (CTX) are freshly prepared in sterile saline. On the day of vector administration (day 0), mice are given cyclophosphamide and methylprednisolone at a dose of 50 mg/kg each via intraperitoneal (IP) injection. Subsequently, weekly IP injections are carried out for 3 weeks to regulate the immune response. Anesthesia was induced with isoflurane at a flow rate of 1 L/min in a chamber. The IP injection site was disinfected with 70% ethanol. Immunosuppressive agents were freshly prepared in sterile saline and administered immediately to maintain potency. After injection, mice were closely monitored for signs of distress or adverse reactions, with their recovery observed until they were fully conscious and mobile.

2.8. Plasma preparation

Blood collection was carried out at 2, 4, 10, and 20 weeks subsequent to injection. The anticoagulation process was accomplished by gathering 90 µL of blood from the tail and instantaneously transferring it into a centrifuge tube filled with 10 µL of 3.2% sodium citrate for blending. The samples were centrifuged at 2000×*g* for 20 minutes at 12°C to separate the plasma. The supernatant was carefully transferred to new microtubes, ensuring that the underlying cell layer was not disturbed, and stored at −80°C until further analysis.[33] For assays, plasma samples were thawed at room temperature and gently mixed to ensure uniformity.

2.9. F8 coagulant activity assay

The coagulant activity of F8 was quantitatively evaluated using a one-stage clotting assay on a Sysmex CA1500 system (Sysmex, Kobe, Japan). Plasma samples were diluted 4 fold to align with the assay's dynamic range and minimum volume requirement. The assay used activated partial thromboplastin time (aPTT) reagent and F8-deficient plasma (OTXW17; Siemens, Marburg, Germany), specifically to assess clotting driven by F8. The sample mixture was then maintained at 37°C to promote thrombin generation and clot formation. Clotting times were recorded by the instrument, and F8 activity was calculated based on a standard curve using human calibration plasma with known F8 activity levels.[34]

2.10. Hepatic function assessment

At the conclusion of the study, hepatic function was assessed to evaluate the biocompatibility of AAV vector treatment. Blood samples were collected from mice under 3% isoflurane anesthesia via retro-orbital bleeding. Post-collection, the blood was incubated at ambient temperature to facilitate clotting for a period of 30 minutes, and subsequently subjected to centrifugation at 1000 g for a duration of 20 minutes at 4°C, a procedure designed to safeguard the serum's pristine condition. The serum was carefully transferred to labeled microtubes and immediately frozen at −80°C to prevent biochemical degradation. Subsequently, the serum was analyzed for the presence of various hepatic enzymes and proteins, including alanine aminotransferase (ALT), albumin (ALB), aspartate aminotransferase (AST), and bilirubin (TBIL), employing diagnostic kits from Beckman Coulter, Inc., (California) and Teco Diagnostics (California), according to the manufacturers' protocols.

2.11. Euthanasia and tissue processing

On completion of the experimental phase, hemophilia A mice were subjected to humane euthanasia through CO_2 induction, followed by verification of death via cervical dislocation, adhering to ethical protocols to minimize suffering. Subsequently, vital organs were harvested promptly to avert autolysis and were immersed in a 10% neutral-buffered formalin solution at ambient temperature to guarantee tissue integrity. Following fixation, tissues underwent a dehydration process using a series of increasing concentrations of alcohol, followed by clearing in xylene before being embedded in paraffin. Histological examination was then conducted on 3 µm sections, which were stained with hematoxylin and eosin to delineate cellular and tissue architecture for detailed scrutiny.

2.12. Statistical analysis

Data are expressed as the mean ± standard error of the mean (SEM). The statistical significance between the experimental and control groups was evaluated using unpaired 2-tailed Student *t* tests. For comparisons across multiple groups, a 1-way analysis of variance (ANOVA) was utilized, complemented by Tukey post-hoc test to discern differences among the various groups. All statistical analyses were executed with GraphPad Prism version 10.2.2 (GraphPad Software, San Diego, CA). A threshold of $P < 0.05$ was applied to determine statistical significance.

3. RESULTS

3.1. Evaluation of human serum ALB signal peptide and CRMs in AAV-mediated gene therapy for hemophilia A

Recent clinical trials have shown promising results using adeno-associated virus serotype 5 (AAV5) vectors for hemophilia A gene therapy.[35,36] Further preclinical studies have assessed various AAV serotypes, including AAV2, AAV5, AAV7, and AAV8, for correcting F8 deficiency in hemophilia A mouse models.[37–40] Among these, AAV8 has demonstrated exceptional efficacy in liver transduction, making it a preferred candidate for gene therapy due to its high transduction efficiency in hepatic cells and rapid uncoating, which enables swift initiation of transgene expression.[41–43] For this study, AAV8 was selected to target liver-specific gene therapy for hemophilia A.

Endothelial cells naturally synthesize F8; however, in gene therapy, hepatocytes are targeted for F8 production due to their

superior protein production capabilities and higher success rate in gene delivery and expression. We hypothesized that using a signal peptide from a highly expressed and secreted hepatocyte gene would enhance the translation, folding, and secretion of F8. Therefore, we utilized the albumin signal peptide (ALBss) to direct F8 secretion in our study.[44]

To test this, we constructed 2 AAV vectors, each driven by the human transthyretin (hTTR) promoter, to express BDDF8 with either the native signal peptide or ALBss. These vectors were administered to a murine model of hemophilia A, and F8 activity (F8%) was measured 2 weeks post-administration. Contrary to expectations and previous studies where ALBss significantly enhanced protein secretion, we observed no significant difference in F8% between the groups, suggesting that the benefits of ALBss may not translate directly from in vitro to the more complex in vivo environment (**Fig. 1A**).

Furthermore, we examined the effect of hepatocyte-specific transcriptional CRMs, identified using a computational strategy,[12] by comparing vectors using the mouse TTR promoter (TTR) with those utilizing a computationally designed enhancer (CRM). Although no statistically significant differences in F8 levels were found between these 2 groups, there was a trend suggesting the potential superiority of CRM-TTR in enhancing F8 expression kinetics and potency (**Fig. 1B**).

3.2. The constructs and expression level of fifteen variants based on AAV8-BDDF8-N6

To optimize the AAV8-BDDF8 vector, we used BDDF8-N6 as the control group, which includes the shortened B-domain—a sequence of 31 amino acids containing 6 N-chain glycosylation recognition sites and the furin cleavage site RHQR. Based on positive outcomes from deleting the RHQR furin recognition site, we explored further amino acid deletions around this site.[45–50] Consequently, 14 variants were designed, ranging from simple deletions like ΔRHQR (removing only RHQR, Vector 1, abbreviated as "V1") to more extensive modifications such as Δ5RHQR23 (deleting RHQR plus five amino acids before and 23 after it, Vector 14, abbreviated as "V14"). Each F8 variant expressing AAV incorporated the CRM-mTTR promoter and ALBss (**Fig. 1C**; Supplementary Figure S1, http://links.lww.com/BS/A107). The detailed sequence information of the expression

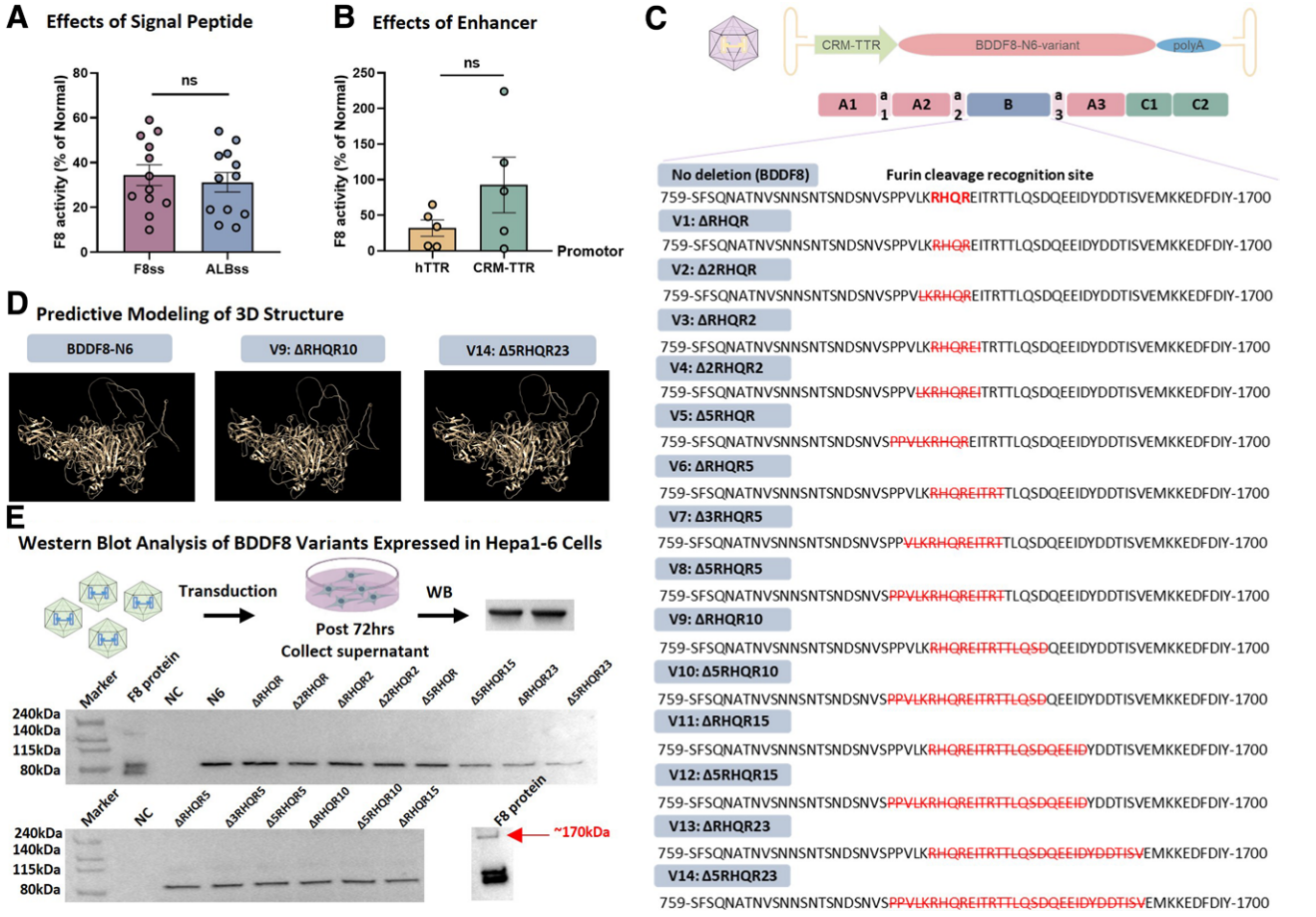

Figure 1. In vitro characterization and optimization of AAV8-BDDF8 vectors for hemophilia A therapy. (A) Evaluation of AAV vectors containing the hTTR promoter and the BDDF8 gene, with and without the ALBss, in hemophilia A mouse models (n = 12). Data are expressed as mean ± SEM, and statistical significance was determined using unpaired 2-tailed Student *t* tests. (B) Comparative analysis of the efficacy of the hTTR and CRM-mTTR promoters in driving gene expression in AAV-mediated gene therapy, assessed in a small cohort (n = 5 mice). Results are presented as mean ± SEM and analyzed with unpaired 2-tailed Student *t* tests. (C) Structural representation of fourteen AAV8-BDDF8-N6 variants, each with specific amino acid deletions within a critical 31 amino acid region near the furin cleavage site, which contains 6 N-linked glycosylation sites. Each variant includes an ALBss for targeted secretion, controlled by the CRM-mTTR promoter to optimize hepatic cell expression. (D) AlphaFold2-based structural predictions comparing the BDDF8-N6 control protein with its derivatives ΔRHQR10 and Δ5RHQR23, highlighting structural conformation differences. (E) Schematic of transduction experiments using AAV-BDDF8 vectors in Hepa1-6 cells over 72 h, followed by collection of supernatants for factor VIII activity measurement and Western blot analysis. Xyntha® BDDF8 protein (170 kDa) was used as a positive control, displaying both full-length and fragmented (heavy and light chains) protein bands (~80 kDa). Hepa1-6 cell supernatant served as the NC. Protein sizes were verified using marker lines. ALBss = albumin signal sequence, BDDF8 = B-domain-deleted FVIII, CRM = cis-acting regulatory modules, hTTR = human transthyretin, NC = negative control.

cassette can be found in Supplementary Figure S2, http://links.lww.com/BS/A107.

3.3. Utilizing AlphaFold2 for structural predictions

Using AlphaFold2,[51] we predicted the structures of the control BDDF8 protein (currently used in clinical trials) and 5 variants with varying degrees of amino acid deletions, including ΔRHQR, Δ5RHQR, ΔRHQR10, Δ5RHQR10, and Δ5RHQR23 (**Fig. 1D**; Supplementary Figure S3B, http://links.lww.com/BS/A107). Structural analysis using the template modeling score (TM score) indicated that even extensive deletions did not significantly alter the protein's structure, suggesting that these modifications may not adversely affect the therapeutic potential of F8. The structural integrity of variants with moderate (eg, ΔRHQR10) and extensive deletions (eg, Δ5RHQR23) was confirmed, with TM scores showing minimal structural deviation from the control (Supplementary Figure S3A, http://links.lww.com/BS/A107). This suggests that deletions around the RHQR site do not significantly disrupt the protein's structure.

3.4. In vitro transfection experiments

In vitro transfection experiments were performed using Hepa1-6 cells and a series of AAV8-BDDF8-N6 variants. After 72 hours, supernatants were collected to quantify F8 protein secretion via a 1-stage clotting assay and Western blot analysis. Surprisingly, no significant differences in F8 expression were observed between the variants, suggesting that the amino acid deletions near the furin recognition site did not significantly affect F8 expression or secretion under the tested conditions (Supplementary Figure S4A, http://links.lww.com/BS/A107).

The Western blot setup included a molecular weight marker in the leftmost lane for accurate band size determination. Adjacent to this, the Xyntha recombinant BDDF8 protein (Pfizer Inc., New York), theoretically sized at 170 kDa and composed of discernible heavy and light chains, was displayed as a reference. The supernatant from Hepa1-6 cells not subjected to AAV transduction served as the negative control. On the right, the lanes were filled with samples from AAV8-BDDF8-N6 and the 14 other AAV-BDDF8 variants, each showing discrete bands at approximately 80 kDa, indicative of the processed and active forms of the protein. Notably, the heavy and light chains of proteins expressed by the variants matched closely in size; for example, the heavy chain in the BDDF8-N6 variant was 85 kDa, while the light chain was 79 kDa (**Fig. 1E**). Due to the presence of 6 glycosylation sites, the light chain exceeded the theoretical weight and appeared to merge with the heavy chain, resulting in a single visible band. No additional bands were observed, confirming the precision of our expression data (**Fig. 1E**).

Quantitative analysis using ImageJ software revealed no statistically significant variations in F8 expression levels across the different variants (Supplementary Figure S4B, http://links.lww.com/BS/A107). This finding indicates that the strategic deletion of amino acids near the furin recognition site did not significantly influence the expression and secretion of F8 in Hepa1-6 cells under the experimental conditions.

3.5. In vivo evaluation of AAV vector efficacy in hemophilia A gene therapy

We further evaluated 14 AAV variants in vivo to treat hemophilia A mice, administered via intravenous injection at a dosage of 2×10^{12} vg/kg body weight. F8 activity was assessed at multiple time points—specifically 2, 4, 10, and 20 weeks post-treatment—to compare the therapeutic potential of each variant over time.

Two weeks post-injection, variants with the most extensive amino acid deletions—specifically variants 13 and 14—showed reduced F8 activity. This reduction suggests that excessive deletions may compromise the protein's function. In contrast, 3 of the remaining 12 variants significantly increased F8 activity, showing 2 to 3 times the normal levels, while the others showed modest increases of 1 to 2 times. Notably, the variant AAV8-BDDF8-ΔRHQR10 was the most effective, achieving F8 activity levels up to 166% 2 weeks post-treatment. Other variants, including Δ2RHQR2, Δ5RHQR, Δ3RHQR5, and ΔRHQR15, also demonstrated substantial F8 activity, ranging from 120% to 150% (**Fig. 2A**).

To confirm the activity assay results, we conducted enzyme-linked immunosorbent assay (ELISA) analysis of serum BDDF8 levels for each variant. The ELISA data (Supplementary Figure S5, http://links.lww.com/BS/A107) show that most variants exhibited BDDF8 expression levels similar to the BDDF8-N6 control, while 4 variants had significantly higher expression levels. Notably, AAV8-BDDF8-ΔRHQR10 exhibited the highest BDDF8 expression, correlating with its superior F8 activity in the activity assays. This consistency between increased F8 activity and elevated BDDF8 protein levels for specific variants further supports the robustness of our findings.

These findings indicate a clear correlation between the extent of amino acid deletion and the bioactivity of the engineered BDDF8 protein. While in vitro experiments and structural predictions suggested that extensive deletions would not significantly alter the protein's structure, the in vivo results show that even subtle structural changes can have considerable functional consequences. This highlights the complex relationship between structural alterations due to amino acid deletions and their impact on the therapeutic efficacy of the protein. Additionally, we observed sex-specific variations in therapeutic outcomes, with male mice consistently showing superior F8 activity compared to female mice. Treated male mice achieved F8 activity levels up to 3 times higher than those in females (**Fig. 2B**).

We also evaluated different AAV vector doses to optimize gene therapy outcomes. The experimental setup included three doses: 5×10^{11}, 1×10^{12}, and 2×10^{12} vg/kg, administered to 8 representative variants of the hemophilia A mouse model. Analysis conducted 2 weeks post-treatment showed that the highest dose of 2×10^{12} vg/kg was the most effective, achieving F8 activity levels between 50% and 100% of normal (**Fig. 2C**). Based on these results, the 2×10^{12} vg/kg dose was selected for further investigation to maximize therapeutic benefits while evaluating long-term efficacy and safety.

A 20-week follow-up study of mice treated with AAV-BDDF8-N6 and its 14 variants revealed that 9 variants maintained F8 activity at approximately 50%. The variant ΔRHQR10 demonstrated sustained performance, with F8 activity levels fluctuating between 50% and 200%. In contrast, variants such as Δ2RHQR, ΔRHQR5, Δ3RHQR5, ΔRHQR23, and Δ5RHQR23 showed a decline in F8 activity to around 20% by the end of week 20 (**Fig. 2D**; Supplementary Figure S6, http://links.lww.com/BS/A107). This decrease mirrors observations from clinical trials, where F8 activity typically declines by up to 80% within 3 years post-treatment. The episomal nature of AAV vectors, which leads to limited genomic integration, contributes to this decline. Since these vectors do not efficiently replicate or transmit to daughter cells during cell division, the expression of therapeutic genes gradually diminishes over time. This pattern, observed in clinical trials, underscores the challenges of maintaining long-term efficacy in gene therapy.

3.6. Safety and long-term efficacy of AAV gene therapy for hemophilia A

To evaluate the clinical applicability of AAV gene therapy for hemophilia A, we examined both its safety and long-term

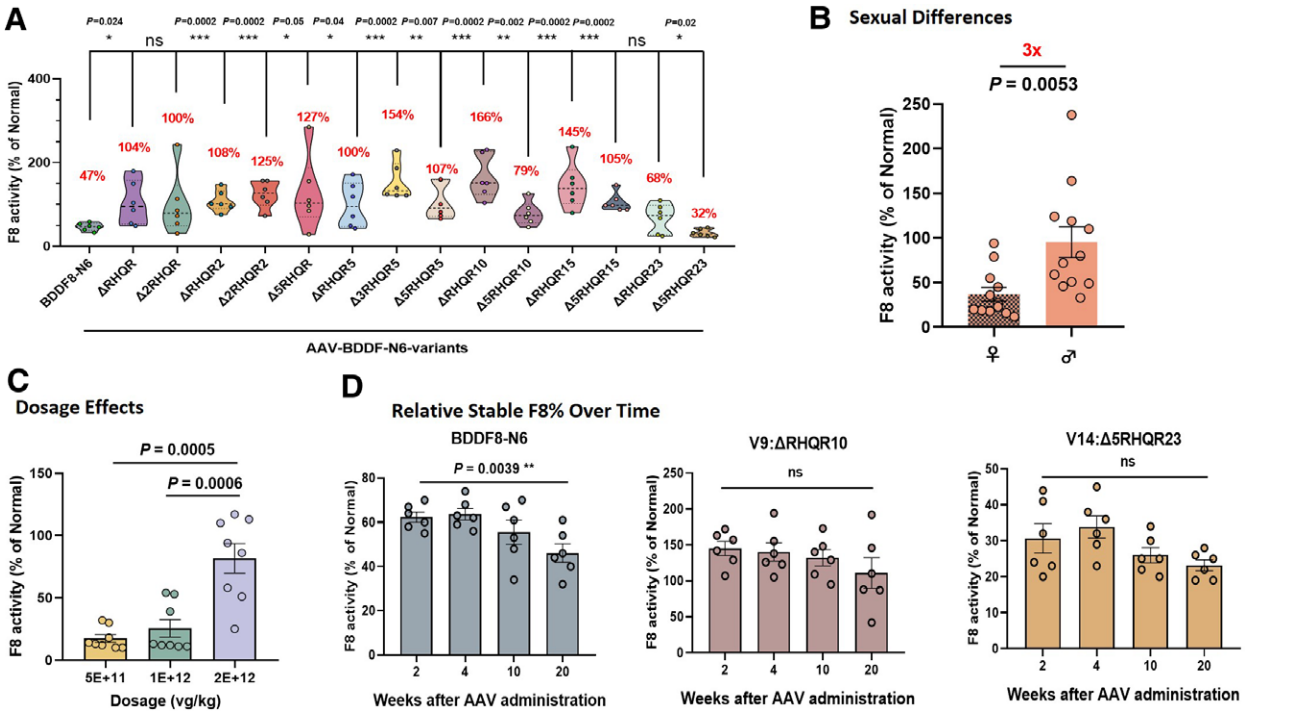

Figure 2. Comprehensive in vivo assessment of AAV vector potency in hemophilia A gene therapy with F8 variants. (A) Post-treatment F8 activity in hemophilia A mice: 14 AAV variants were administered intravenously at a dose of 2×10^{12} vg/kg (n = 6). The ΔRHQR10 variant showed significantly higher efficacy, while the Δ5RHQR23 variant exhibited reduced activity. (B) Sex-based efficacy differences: male mice exhibited F8 activity levels 3 times higher than those in female mice (n = 12). (C) Dosage optimization in AAV therapy: 3 different dosages (5×10^{11}, 1×10^{12}, and 2×10^{12} vg/kg) were tested. The highest dosage consistently resulted in the best outcomes, with F8 activity reaching 50% to 100% of normal levels at the 2-wk time point. This section involved 8 variants, each tested in 3 mice. (D) Long-term treatment efficacy: F8 activity was monitored at 2, 4, 10, and 20 wk post-treatment to evaluate the sustained therapeutic effects (n = 6). Data are presented as mean ± SEM and were analyzed using unpaired 2-tailed Student *t* tests. AAV = adeno-associated virus, SEM = standard error of the mean.

efficacy. In our study, we conducted detailed assessments of liver function and histopathology to identify potential adverse effects after long-term expression of F8. Twenty weeks post-treatment, we sacrificed a cohort of mice randomly selected from each variant group for analysis.

Hematoxylin and eosin (H&E) staining was performed on liver sections to assess anatomical changes or damage. The results showed no significant differences in liver morphology between treated and untreated mice, indicating that AAV-mediated gene therapy did not cause histopathological abnormalities (**Fig. 3A**). Additionally, we measured serum markers associated with liver damage, including AST, ALT, total TBIL, and total ALB. These markers remained within normal ranges in both treated and control groups, further supporting the safety of this therapeutic approach (**Fig. 3B**).

These findings collectively suggest that AAV8-BDDF8 gene therapy for hemophilia A is well-tolerated in mice, with no evidence of significant liver toxicity or morphological changes over an extended period. This positive safety profile is crucial for advancing AAV-based therapies toward clinical use and provides a strong foundation for future studies to confirm these results in human trials.

4. DISCUSSION

This study represents a significant advancement in hemophilia A treatment through the development of novel F8 variants that enhance in vivo activity following AAV-mediated liver-targeted therapy. Unlike conventional approaches that focus on identifying natural mutants or extending the B-domain, our strategy involved extensive amino acid deletions around the furin recognition site. These deletions were inspired by previous research but extended further to explore their effects on protein efficacy. Our in vivo findings suggest that appropriate deletions can enhance F8 activity, implying that shortened constructs may improve packaging of the full-length AAV genome. Although this hypothesis requires further validation, it offers a promising avenue for enhancing gene therapy efficiency.

Structural predictions using AlphaFold2, followed by in vitro cell transduction and Western blot analysis, revealed no significant differences among the shortened variants. However, in vivo studies showed subtle yet important differences, with variants like AAV8-BDDF8-ΔRHQR10 demonstrating significant increases in F8 activity, underscoring the potential of these engineered constructs to improve therapeutic outcomes. Quantitative analysis of F8 protein expression in Hepa1-6 cells confirmed the in vitro efficacy of AAV8-BDDF8 variants, with consistent expression levels across variants, indicating that these modifications do not compromise the protein's expression capacity. These findings, supported by in vivo activity trends, challenge conventional assumptions about the relationship between protein structure and function, emphasizing the importance of empirical validation in therapeutic development.

Our findings offer a new perspective on enhancing protein secretion efficiency and gene expression kinetics in gene therapy. While previous studies suggested potential benefits from modifications like the human serum ALB signal peptide and CRMs, our results show no significant improvement in F8 activity in a hemophilia A mouse model, suggesting that the complexity of the in vivo environment may dampen expected enhancements. Additionally, our experiments highlighted the potential superiority of species-specific promoters, such as the CRM-mTTR promoter, which could provide more effective transcriptional control than its human counterpart. This observation is crucial for translating gene therapy from laboratory findings to

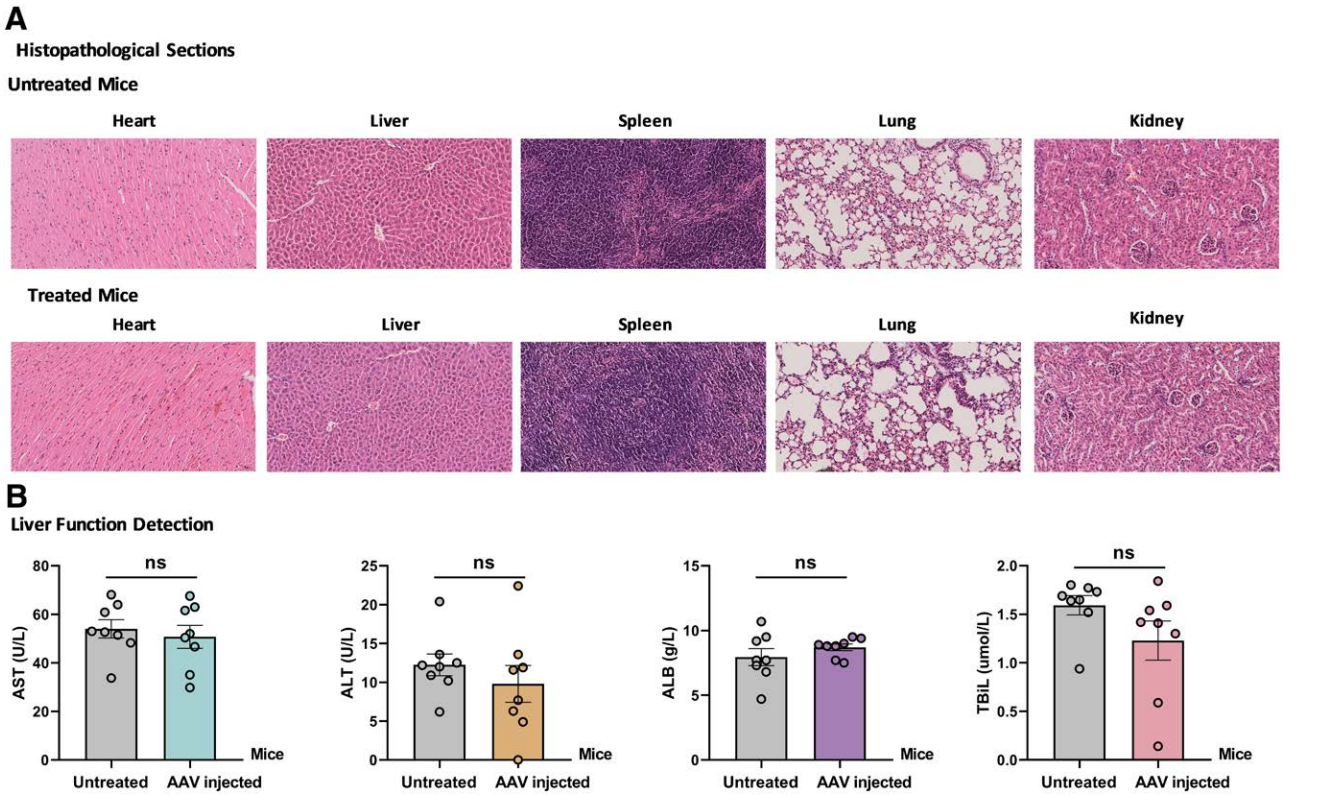

Figure 3. Safety assessment following AAV gene therapy in hemophilia A mice. (A) Histological evaluation: liver tissues were examined using H&E staining 20 wk post-treatment with AAV8-BDDF8. No significant histopathological differences were observed between treated and untreated mice, suggesting the absence of adverse tissue alterations. (B) Liver function markers: serum levels of AST, ALT, ALB, and TBIL were measured. No significant differences were found between treated mice (n = 6) and control mice (n = 3), indicating no liver damage. Statistical analyses were performed using 1-way ANOVA and unpaired 2-tailed Student *t* tests. AAV = adeno-associated virus, ALB = albumin, ALT = alanine aminotransferase, ANOVA = 1-way analysis of variance, AST = aspartate aminotransferase, BDDF8 = B-domain-deleted FVIII, H&E = hematoxylin and eosin, TBIL = total bilirubin.

practical in vivo applications and underscores the need for further investigation into the mechanisms governing protein secretion and gene regulation in physiological contexts.

Additionally, the identification of sex-specific differences in response to AAV therapy, with male mice exhibiting better outcomes, is significant given the X-linked inheritance pattern of hemophilia A. These findings could inform future gender-specific treatment strategies, improving the precision and effectiveness of gene therapies.

The long-term safety assessment of AAV gene therapy in our study is particularly encouraging. Observations showing no significant differences in liver function markers or histopathological changes between treated and untreated mice reinforce the safety profile of AAV vectors for hemophilia A gene therapy. These findings strengthen confidence in their potential clinical application and provide a solid foundation for future therapeutic strategies. Moreover, sustained F8 activity in mice treated with AAV-BDDF8-N6 and its variants over a 20-week period demonstrates the durability of these gene therapy vectors, significantly reducing bleeding events and improving the quality of life for hemophilia A models.

The findings from our study on optimizing AAV8-BDDF8 vector configurations for hemophilia A therapy are pivotal for advancing the field of gene therapy. By demonstrating enhanced F8 expression and stable liver function post-treatment, our research strongly supports the use of tailored AAV vectors in clinical settings, particularly in light of recent U.S. Food and Drug Administration (FDA) approvals of gene therapies for blood disorders. Furthermore, the methodologies and insights from this study have broader implications, potentially influencing treatment strategies for a range of genetic disorders involving protein deficiency or dysfunction. Our approach can refine vector design and promoter usage, improving both the efficacy and safety profiles of gene therapies for diseases like muscular dystrophy and cystic fibrosis.

However, several limitations must be acknowledged. The hemophilia A mouse model, while invaluable for preliminary testing, does not fully replicate the human condition, particularly in terms of immune responses and long-term reactions to gene therapy. Thus, cautious extrapolation of our findings to clinical settings is necessary. Further validation in larger animal models, such as dogs or non-human primates, is crucial before clinical trials can proceed. Additionally, the dosing parameters established for mice need to be adjusted for humans, necessitating extensive dose-escalation studies to determine the safest and most effective dosage.

Long-term safety and efficacy have yet to be fully established, with ongoing research needed to assess potential adverse effects and strategies for inducing tolerance to the F8 protein. Furthermore, exploring alternative gene-editing technologies, such as CRISPR-Cas systems, may offer more permanent solutions. Evaluating the immunogenicity of both the vector and transgene in diverse genetic backgrounds is also crucial to ensure the broad applicability of the therapy.

In summary, the optimized AAV8-BDDF8 vector shows significant promise for improving hemophilia A therapy and lays the foundation for future research in gene therapy. Continued exploration and clinical validation of these findings could lead to transformative advances in the treatment of genetic disorders, ultimately improving patient outcomes and quality of life. As gene therapy continues to evolve, the insights from this study will likely influence a broad range of therapeutic developments,

fostering innovation and the adoption of new technologies in clinical practice.

ACKNOWLEDGMENTS

This work was supported by the National Key Research and Development Program of China (Grant Nos. 2019YFA0110803, 2019YFA0110204, 2019YFA0110802, and 2021YFA1100900), the National Natural Science Foundation of China (Grant Nos. 82402188, 81870149, 82070115, 81770198, 81890990, and 81730006), the Chinese Academy of Medical Sciences (CAMS) Innovation Fund for Medical Sciences (CIFMS) (Grant Nos. 2024-I2M-3-018, 2023-I2M-2-007, 2022-I2M-2-001, 2022-I2M-2-003, 2021-I2M-1-041, 2021-I2M-1-040, and 2021-I2M-1-001), the Non-profit Central Research Institute Fund of Chinese Academy of Medical Sciences (Grant No. 2020-PT310-011), the Tianjin Synthetic Biotechnology Innovation Capacity Improvement Project (Grant No. TSBICIP-KJGG-017), the CAMS Fundamental Research Funds for Central Research Institutes (Grant No. 3332021093), the Haihe Laboratory of Cell Ecosystem Innovation Fund (Grant Nos. 24HHXBSS00005 and HH22KYZX0022), and the State Key Laboratory of Experimental Hematology Research Grant (Grant No. Z23-05).

ETHICAL APPROVAL

The mice were housed at the State Key Laboratory of Experimental Hematology (SKLEH) in Tianjin, China. All animal procedures were conducted in accordance with protocols approved by the Institutional Animal Care and Use Committee of SKLEH and the Institute of Hematology, with the ethical approval number CIFMS2024003-EC-1. Euthanasia was carried out using inhalation anesthesia followed by dislocation of the cervical vertebrae. Initially, mice were placed in an induction chamber and exposed to isoflurane. The concentration of anesthetic gas was carefully adjusted to ensure complete unconsciousness and absence of response to external stimuli. Subsequently, the cervical vertebrae were swiftly and completely dislocated to minimize any potential pain or distress to the mice.

AUTHOR CONTRIBUTIONS

X.-B.Z., J.-J.Z., and S.-N.T. designed the experiments. J.-J.Z., S.-N.T., X.L., M.Z., and Z.-Y.P. were responsible for data acquisition. G.-H.L. and F.Z. conducted vector construction and AAV packaging. Data analysis and interpretation were carried out by J.-J.Z., S.-N.T., and X.-B.Z., with statistical analysis contributed by J.-J.Z. and S.-N.T. The manuscript was written by X.-B.Z., J.-J.Z., and S.-N.T., with administrative support and supervision provided by X.-B.Z. and J.-P.Z. All authors reviewed and approved the manuscript for submission and publication.

REFERENCES

[1] Srivastava A, Brewer AK, Mauser-Bunschoten EP, et al. Guidelines for the management of hemophilia. *Haemophilia* 2013;19(1):e1–47.
[2] Hoyer LW. Hemophilia A. *N Engl J Med* 1994;330(1):38–47.
[3] Mannucci PM, Tuddenham EGD. The hemophilias—from royal genes to gene therapy. *N Engl J Med* 2001;344(23):1773–1779.
[4] Nogami K, Shima M. New therapies using nonfactor products for patients with hemophilia and inhibitors. *Blood*. 2019;133(5):399–406.
[5] Astermark J, Donfield SM, DiMichele DM, et al. A randomized comparison of bypassing agents in hemophilia complicated by an inhibitor: the FEIBA NovoSeven Comparative (FENOC) Study. *Blood* 2006;109(2):546–551.
[6] Franchini M, Mannucci PM. Hemophilia A in the third millennium. *Blood Rev* 2013;27(4):179–184.
[7] Wang D, Tai PWL, Gao G. Adeno-associated virus vector as a platform for gene therapy delivery. *Nat Rev Drug Discov* 2019;18(5):358–378.
[8] Hareendran S, Balakrishnan B, Sen D, Kumar S, Srivastava A, Jayandharan GR. Adeno-associated virus (AAV) vectors in gene therapy: immune challenges and strategies to circumvent them. *Rev Med Virol* 2013;23(6):399–413.
[9] Wang L, Yang Y, Breton CA, et al. CRISPR/Cas9-mediated in vivo gene targeting corrects hemostasis in newborn and adult factor IX-knockout mice. *Blood* 2019;133(26):2745–2752.
[10] He X, Zhang Z, Xue J, et al. Low-dose AAV-CRISPR-mediated liver-specific knock-in restored hemostasis in neonatal hemophilia B mice with subtle antibody response. *Nat Commun* 2022;13(1):7275.
[11] Jayandharan GR, Zhong L, Sack BK, et al. Optimized adeno-associated virus (AAV)–protein phosphatase-5 helper viruses for efficient liver transduction by single-stranded AAV vectors therapeutic expression of factor IX at reduced vector doses. *Hum Gene Ther* 2010;21(3):271–283.
[12] Nair N, Rincon MY, Evens H, et al. Computationally designed liver-specific transcriptional modules and hyperactive factor IX improve hepatic gene therapy. *Blood* 2014;123(20):3195–3199.
[13] Chuah MK, Petrus I, De Bleser P, et al. Liver-specific transcriptional modules identified by genome-wide in silico analysis enable efficient gene therapy in mice and non-human primates. *Mol Ther* 2014;22(9):1605–1613.
[14] Mnyandu N, Limani SW, Arbuthnot P, Maepa MB. Advances in designing Adeno-associated viral vectors for development of anti-HBV gene therapeutics. *Virol J* 2021;18(1):247.
[15] Samelson-Jones BJ, Arruda VR. Protein-engineered coagulation factors for hemophilia gene therapy. *Mol Ther Methods Clin Dev* 2019;12:184–201.
[16] Wu Z, Yang H, Colosi P. Effect of genome size on AAV vector packaging. *Mol Ther* 2010;18(1):80–86.
[17] Pahl S, Pavlova A, Driesen J, Oldenburg J. Effect of F8 B domain gene variants on synthesis, secretion, activity and stability of factor VIII protein. *Thromb Haemost* 2014;111(1):58–66.
[18] Pipe SW. Functional roles of the factor VIII B domain. *Haemophilia* 2009;15(6):1187–1196.
[19] Nichols WC, Seligsohn U, Zivelin A, et al. Mutations in the ER–Golgi intermediate compartment protein ERGIC-53 cause combined deficiency of coagulation factors V and VIII. *Cell* 1998;93:61–70.
[20] Moussalli M, Pipe SW, Hauri HP, Nichols WC, Ginsburg D, Kaufman RJ. Mannose-dependent endoplasmic reticulum (ER)-Golgi intermediate compartment-53-mediated ER to Golgi trafficking of coagulation factors V and VIII. *J Biol Chem* 1999;274(46):32539–32542.
[21] Zhang B, Cunningham MA, Nichols WC, et al. Bleeding due to disruption of a cargo-specific ER-to-Golgi transport complex. *Nat Genet* 2003;34:220–225.
[22] Wen W, Quan ZJ, Li SA, et al. Effective control of large deletions after double-strand breaks by homology-directed repair and dsODN insertion. *Genome Biol* 2021;22(1):236.
[23] Quan ZJ, Li SA, Yang ZX, et al. GREPore-seq: a robust workflow to detect changes after gene editing through long-range PCR and nanopore sequencing. *Genomics Proteomics Bioinformatics* 2023;21:1221–1236.
[24] Li G, Tian S, Sun X, et al. Leveraging CRISPR-Cas9 for accurate detection of AAV-neutralizing antibodies: the AAV-HDR method. *Hum Gene Ther* 2024;35:490–505.
[25] Fu YW, Dai XY, Wang WT, et al. Dynamics and competition of CRISPR-Cas9 ribonucleoproteins and AAV donor-mediated NHEJ, MMEJ and HDR editing. *Nucleic Acids Res* 2021;49(2):969–985.
[26] Yang Z, Fu Y, Zhao J, et al. Superior fidelity and distinct editing outcomes of SaCas9 compared to SpCas9 in genome editing. *Genomics Proteomics Bioinformatics* 2023;21(6):1206–1220.
[27] Mirdita M, Schutze K, Moriwaki Y, Heo L, Ovchinnikov S, Steinegger M. ColabFold: making protein folding accessible to all. *Nat Methods* 2022;19(6):679–682.
[28] Zhang Y, Skolnick J. TM-align: a protein structure alignment algorithm based on the TM-score. *Nucleic Acids Res* 2005;33(7):2302–2309.
[29] Xu J, Zhang Y. How significant is a protein structure similarity with TM-score = 0.5? *Bioinformatics* 2010;26(7):889–895.
[30] Zhang Y. Progress and challenges in protein structure prediction. *Curr Opin Struct Biol* 2008;18(3):342–348.
[31] Schneider CA, Rasband WS, Eliceiri KW. NIH Image to ImageJ 25 years of image analysis. *Nat Methods* 2012;9(7):671–675.
[32] Zhang JP, Cheng XX, Zhao M, et al. Curing hemophilia A by NHEJ-mediated ectopic F8 insertion in the mouse. *Genome Biol* 2019;20(1):276.
[33] Zhao M, Sun YD, Yin M, et al. Modulation of immune reaction in hydrodynamic gene therapy for hemophilia A. *Hum Gene Ther* 2022;33(7–8):404–420.

[34] Zhao JJ, Sun XY, Tian SN, et al. Decoding the complexity of on-target integration: characterizing DNA insertions at the CRISPR-Cas9 targeted locus using nanopore sequencing. *BMC Genomics* 2024;25(1):189.
[35] Rangarajan S, Walsh L, Lester W, et al. AAV5-factor VIII gene transfer in severe hemophilia A. *N Engl J Med* 2017;377(26):2519–2530.
[36] Pasi KJ, Rangarajan S, Mitchell N, et al. Multiyear follow-up of AAV5-hFVIII-SQ gene therapy for hemophilia A. *N Engl J Med* 2020;382(1):29–40.
[37] Nathwani AC, Gray JT, Ng CY, et al. Self-complementary adeno-associated virus vectors containing a novel liver-specific human factor IX expression cassette enable highly efficient transduction of murine and nonhuman primate liver. *Blood* 2006;107(7):2653–2661.
[38] Wang L, Bell P, Lin J, Calcedo R, Tarantal AF, Wilson JM. AAV8-mediated hepatic gene transfer in infant rhesus monkeys (Macaca mulatta). *Mol Ther* 2011;19(11):2012–2020.
[39] Mingozzi F, High KA. Immune responses to AAV vectors: overcoming barriers to successful gene therapy. *Blood* 2013;122(1):23–36.
[40] George LA, Sullivan SK, Giermasz A, et al. Hemophilia B gene therapy with a high-specific-activity factor IX variant. *N Engl J Med* 2017;377(23):2215–2227.
[41] Sarkar R, Tetreault R, Gao G, et al. Total correction of hemophilia A mice with canine FVIII using an AAV 8 serotype. *Blood* 2004;103(4):1253–1260.
[42] Nathwani AC, Reiss UM, Tuddenham EG, et al. Long-term safety and efficacy of factor IX gene therapy in hemophilia B. *N Engl J Med* 2014;371(21):1994–2004.
[43] Sen D, Gadkari RA, Sudha G, et al. Targeted modifications in adeno-associated virus serotype 8 capsid improves its hepatic gene transfer efficiency in vivo. *Hum Gene Ther Methods* 2013;24(2):104–116.
[44] Attallah C, Etcheverrigaray M, Kratje R, Oggero M. A highly efficient modified human serum albumin signal peptide to secrete proteins in cells derived from different mammalian species. *Protein Expr Purif* 2017;132:27–33.
[45] Siner JI, Samelson-Jones BJ, Crudele JM, et al. Circumventing furin enhances factor VIII biological activity and ameliorates bleeding phenotypes in hemophilia models. *JCI Insight*. 2016;1(16):e89371.
[46] Sabatino DE, Freguia CF, Toso R, et al. Recombinant canine B-domain–deleted FVIII exhibits high specific activity and is safe in the canine hemophilia A model. *Blood* 2009;114(20):4562–4565.
[47] Siner JI, Iacobelli NP, Sabatino DE, et al. Minimal modification in the factor VIII B-domain sequence ameliorates the murine hemophilia A phenotype. *Blood* 2013;121(21):4396–4403.
[48] Miao HZ, Sirachainan N, Palmer L, et al. Bioengineering of coagulation factor VIII for improved secretion. *Blood* 2004;103(9):3412–3419.
[49] Cerullo V, Seiler MP, Mane V, et al. Correction of murine hemophilia A and immunological differences of factor VIII variants delivered by helper-dependent adenoviral vectors. *Mol Ther* 2007;15(12):2080–2087.
[50] McIntosh J, Lenting PJ, Rosales C, et al. Therapeutic levels of FVIII following a single peripheral vein administration of rAAV vector encoding a novel human factor VIII variant. *Blood* 2013;121(17):3335–3344.
[51] Jumper J, Evans R, Pritzel A, et al. Highly accurate protein structure prediction with AlphaFold. *Nature* 2021;596(7873):583–589.